Polymerization of Liquid Propylene with a Fourth-Generation Ziegler–Natta Catalyst: Influence of Temperature, Hydrogen, Monomer Concentration, and Prepolymerization Method on Powder Morphology

Jochem T. M. Pater,[1] Günter Weickert,[2] Wim P. M. van Swaaij[2]

[1] *BP Chemicals SNC, Research and Technology center, Ecopolis Lavera Sud, P. O. Box 6, F-13117, Lavéra, France*
[2] *Process Technology Institute Twente, University of Twente, High Pressure Laboratories, P. O. Box 217, NL-7500AE Enschede, The Netherlands*

Received 29 August 2001; accepted 5 June 2002

ABSTRACT: Liquid propylene was polymerized in a 5-L autoclave batch reactor using a commercially available $TiCl_4/MgCl_2/Al(ethyl)_3$/DCPDMS Ziegler–Natta catalyst, with a phthalate ester as internal electron donor. The powders from these polymerizations were characterized using laser diffraction particle size distribution (PSD) analysis, scanning electron microscopy (SEM), and bulk density measurements. These characteristics were analyzed as a function of the process conditions, including hydrogen and monomer concentration, polymerization temperature, and the prepolymerization method. It was shown that polymerization temperature influences the powder morphology to a large extent. At low temperatures, high-density particles were obtained, showing regular shaped particle surfaces and low porosities. With increasing temperature, the morphology gradually was transferred into a more open structure, with irregular surfaces and poor replication of the shape of the catalyst particle. When using a prepolymerization step at a relatively low temperature, the morphology obtained was determined by this prepolymerization step and was independent from conditions in main polymerization. The morphology obtained was the same as that observed after a full polymerization at temperature. Even when using a short polymerization at an increasing temperature, the morphology was strongly influenced by the initial conditions. The effect of variation in hydrogen concentration supported the conclusion that the initial polymerization rate determines the powder morphology. In the absence of hydrogen, high bulk densities, and regularly shaped particles were obtained, even at high temperatures. With increasing hydrogen concentration, the reaction rates increased rapidly, and with that changed the morphology. © 2002 Wiley Periodicals, Inc. J Appl Polym Sci 87: 1421–1435, 2003

Key words: polymerization; propylene; morphology; hydrogen; liquid pool; morphogenesis; prepolymerization; Ziegler–Natta

INTRODUCTION

Since the first successful attempts to produce isotactic polypropylene in the laboratories of Natta, a number of new catalyst systems have been developed. Natta's $TiCl_3/AlEt_2Cl$ catalyst can be considered as a "first generation," and over the years four more generations of Ziegler–Natta (ZN) catalysts have been developed. Parallel to this continuous evolution of the ZN catalyst, the metallocenes—sometimes called the sixth-generation catalysts—have been developed and implemented in industrial processes. But despite some clear advantages of these new metal-organic components, and in contrast with almost all predictions made in the last two decades on the future of metallocenes, the vast majority of the world's polypropylene production is based on ZN catalysis, typically the third- and fourth-generation catalysts.

These new designs of the conventional catalyst systems are used in all the different industrial processes for polypropylene. Because of the fact that the modern processes typically involve a cascade of polymerization reactors, varying from the bulk–gas phase combination in Basell's Spheripol to the series of gas phase compartments in bp's PP-Innovene (formerly known as Amoco process; PP: polypropylene), the powder morphology of the polymer product is of great importance. First, the particle shape determines its behavior in the reactors, especially in the fluidized bed gas phase systems. Secondly, the distribution of the rubbery components in the production of high impact polypropylene in the i-PP matrix is, to a large extent determined by the morphology of catalyst and polymer powders. Finally, the absence of fines prevents reactor fouling and the absence of coarse particles eliminates undesirable fluidization and agglomeration effects.

Correspondence to: J. T. M. Pater (Jochem.Pater@fr. bp.com).
Contract grant sponsor: The Dow Chemical Company, Freeport, TX, USA.

Journal of Applied Polymer Science, Vol. 87, 1421–1435 (2003)

Of course, an optimal polymer particle morphology is one of the important goals in catalyst development. Next to that, also the polymerization process itself can influence and change the powder morphology. Process conditions determine the reaction rates and with that the powder morphology, but also physical stress on the particle due to for example stirrer action can change this morphology.

Control of particle morphology is based on the fact that the polymer tends to replicate the shape of the catalyst particle on which it is produced. To be able to understand the process of shape replication, one should understand the growth mechanism of the particle. It is well accepted that growth of the particle shows the following characteristics in the Ziegler–Natta catalyzed olefin polymerizations:

- In the initial stage of the polymerization, the catalyst particle breaks up into a large number of smaller catalyst fragments. During the polymerization the size of these fragments decreases due to further fragmentation.
- The entangled polymer produced keeps the different fragments together and forms the continuous phase in the growing particle very soon after the start of fragmentation.[1]
- After full fragmentation, the small fragments are well distributed over the growing particle. Polymer production occurs on all the catalyst fragments.

With these characteristics, particle growth is believed to show replication of the shape of the catalyst particle. However, it is shown[2–5] that there are some requirements with respect to catalyst structure and reaction conditions to show uniform catalyst fragmentation. The catalyst needs to be highly porous to allow the monomer to flow into the center of the particle, and to ensure a large number of possible crack positions. The catalyst structure must have a mechanical strength high enough to withstand handling, but low enough to break in polymerization conditions. Of course, active sites should be well distributed over the catalyst to ensure an even distribution of polymer production over the catalyst.[6] Furthermore, polymerization conditions should be chosen in such a way that mass transfer limitations are not likely to occur, to ensure even polymerization across the particle. This is well demonstrated in the "Reactor Granule Technology" of Himont/Montecatini, where the spherical polymer granule is formed with high porosity to allow copolymerization for polyolefin alloys.[7]

The growth model of these particles has been modeled by a large number of scientists over the past years, where the Multi Grain Model (MGM) is the most well known.[8–12] It should be realized that in the MGM model, the fragmentation is assumed to be complete at time zero and catalyst fragments are assumed to be equal in size. The group of Chiovetta has worked intensively in the early 1990s on implementation of the fragmentation step in single particle models. Their aim was to demonstrate its effect on the transfer of heat and mass to and from the particle,[13–17] rather than describing its effect on morphology development.

Until now it has not been possible to develop models that are able to describe and predict particle morphology as a function of reaction conditions and recipe. The reason for this is that the fragmentation of the catalyst is a very complex process, depending on a large number of variables like local initial polymerization rates and crystallization of the polymer product. We think that, to be able to develop such models, one needs full understanding of the different processes playing a role in the development of the internal and external shape of the particle. This is possible with the combination of model development with experimental data of real polymerizations. In the recent past some groups attempted to clarify the particle growth mechanisms—for example, Noristi et al.,[18] Kakugo et al.,[19,20] and Ferrero[21] These studies are hard to generalize, as the behavior of the system will also depend on the type of the catalyst used and the type of polymer formed. For example, Han-Adebekun et al. studied the effect of reaction conditions on polymer particle morphology, and showed that the influence of temperature and comonomer composition on particle morphology were sintering effects due to polymer melting.[22,23]

Recently, two interesting experimental studies on PP morphology were published. Cecchin et al.[24] studied the homo- and copolymerization of propylene, using a spherical Ziegler–Natta catalyst. To describe the particle growth, they proposed mechanism that entails the features of both a dual grain and a polymeric flow system: the monomer polymerizes at the surface of the catalyst microparticles forming a polymer shell around each of them. These polymer microglobules form larger agglomerates, which tend to behave as individual polymeric flow units. Furthermore, the work of Kittilsen and McKenna[25] shows how powerful relatively simple experiments at intelligently chosen conditions can be. They confirmed the model for the formation of electron paramagnetic resonance (EPR) on PP particles: the EPR initially form underneath the PP produced in the first stage of the reaction, and then seeps out to partially fill the micropores of the host matrix.

We think that by systematically varying reaction conditions and recipes, in boundaries far wider than the industrial relevant operation window and by analyzing the powders from these tests, the basic mechanisms creating particle morphology can be further revealed.

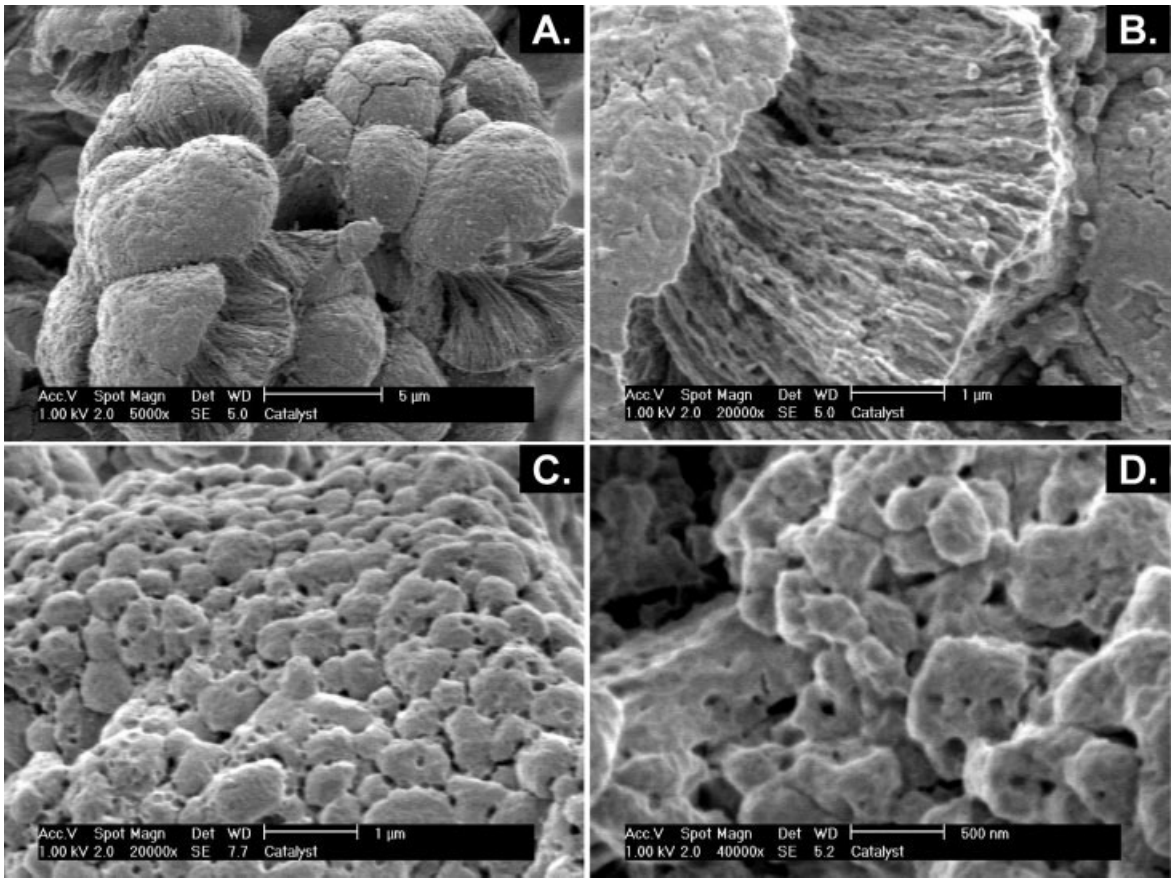

Figure 1 Scanning electron microscopy (SEM) pictures of the nonactivated catalyst material before polymerization.

In this work we study powders from the polymerization of liquid propylene using a highly active Ziegler–Natta catalyst. The relations between process conditions like polymerization temperature, the application of a prepolymerization step, the monomer concentration, the hydrogen concentration, and the morphology of the produced powder are discussed.

EXPERIMENTAL

Chemicals

Catalyst system

The catalyst system used here was a commercially available Ziegler–Natta catalyst of the fourth generation as defined by Moore,[26] with $TiCl_4$ on a $MgCl_2$ support. Triethyl aluminum was used as a cocatalyst and the so-called D-donor (di-cyclopentyl di-methoxy silane) was used as external electron donor for regulation of the stereospecificity. A phthalate ester was used as internal electron donor. Figure 1 shows electron microscopy pictures of the highly porous catalyst material. In these pictures it can be seen that the catalyst particles are built from 20 to 30 spherical shaped subparticles. The particle size distribution of the catalyst is shown in Figure 2. The relatively narrow particle size distribution shows an average particle size of 24.4 μm. The titanium concentration at the catalyst was 1.54 wt %.

In all polymerization tests, the Al/Ti and Al/Si ratios were kept constant at values of 735 and 45, respectively, and typically 10 mg of catalyst was used.

Monomer, hydrogen, nitrogen, and hexane

The propylene used in the experiments was of so-called "polymer grade" and obtained from Indugas, with a purity>99.5%, with propane as main impurity. The hydrogen and nitrogen used were of >99.999% purity. Table I shows the different chemicals used, their origin, the purity and the finishing purification steps. The hexane added to the system was of "Pro Analysi" quality obtained from Merck.

The hydrogen, nitrogen, and hexane were further purified by passing them over a reduced copper catalyst and subsequently passing through three different beds of molecular sieves, with pore sizes of 13, 4, and 3 Å, respectively. The copper catalyst was obtained from BASF. The propylene was purified in the same way, after it was passed over a bed of oxidized copper catalyst to remove carbon monoxide.

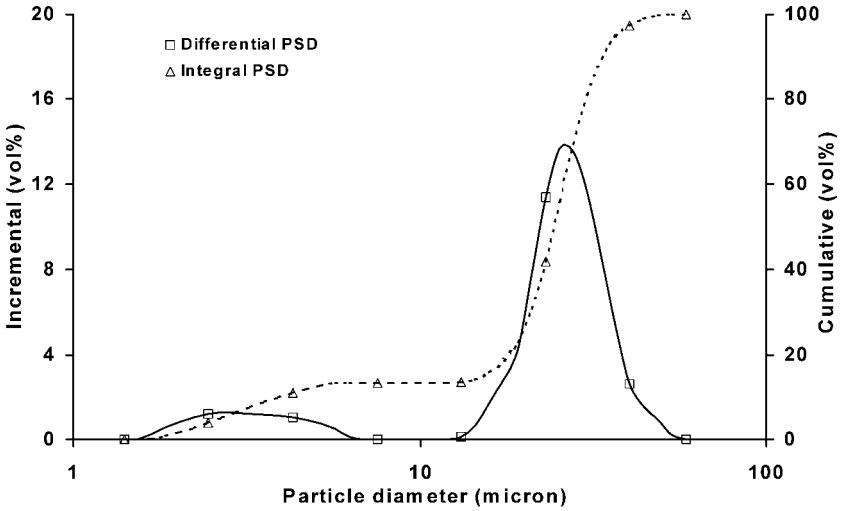

Figure 2 Particle size distribution of the catalyst before polymerization.

Polymerization methods

The procedure and hardware used in the polymerization experiments presented here was described by us recently[27,28] in more detail. Reactions were carried out in a 5-L stainless steel Büchi BEP 280 reactor with a six-blade impeller type stirrer at 2000 rpm. Cooling water in the jacket was used to maintain isothermal conditions during the experiment. The reactor setup is schematically shown in Figure 3.

Catalyst preparation

The catalyst was prepared in a Braun 150 B-G-II glove box under a nitrogen atmosphere. The oil suspended catalyst was weighed in a vial and diluted with some hexane. In another vial the desired amounts of tri ethyl aluminum (TEA) and D-donor were precontacted at room temperature, diluted in hexane. The catalyst was not activated before injection to the polymerization reactor.

Reactor preparation

To purify the reactor, it was flushed with nitrogen before every polymerization experiment, at a reactor wall temperature of about 95°C. The reactor was subsequently evacuated for about 5 min. This procedure was repeated at least 5 times. After this flushing procedure, the reactor was tested for leakage with hydrogen at 20 bar. Then the reactor was evacuated and flushed a few times with gaseous propylene to wash out the hydrogen. Then the desired amounts of hydrogen and propylene were fed to the system, typically being 31.6 mole of propylene.

Polymerization procedure

After the system had reached the desired initial temperature, the TEA/donor/hexane mixture was injected to the reactor. The vial was washed with fresh hexane two times to ensure that all cocatalyst and donor was introduced. Subsequently, about 1 min af-

TABLE I
The Different Components Used in the Polymerization Experiments, with Their Origin, Their Purity, and the Final Treatment Before Use

Component	Supplier	Purity	Further Processing
TEAL	AkzoNobel	>96%, AIH3 <0.07%	None
Nitrogen	PraxAir	>99.999%, <4 vpm H_2O, <4 vpm O_2, <1 vpm CO_2	3A, 4A, 13X mole sieves, red-ed BTS cat.
Hydrogen	PraxAir	>99.999%, <5 vpm H_2O, <1 vpm O_2, <0.5 vpm CO	3A, 4A, 13X mole sieves, red-ed BTS cat.
Propylene	Prax Air	<20 wt ppm H_2O, <5 wt ppm CO_2, < 0.5 wt ppm CO	3A, 4A, 13X mole sieves, ox-ed + red-ed BTS
Hexane	Merck	>99%, <0.01%H_2O, <0.05% S compounds	3A, 4A, 13X mole sieves, reduced BTS cat.
D-donor	Dow Chem.		
Mole sieves	Aldrich	NA	NA
BTS cat	BASF	NA	NA

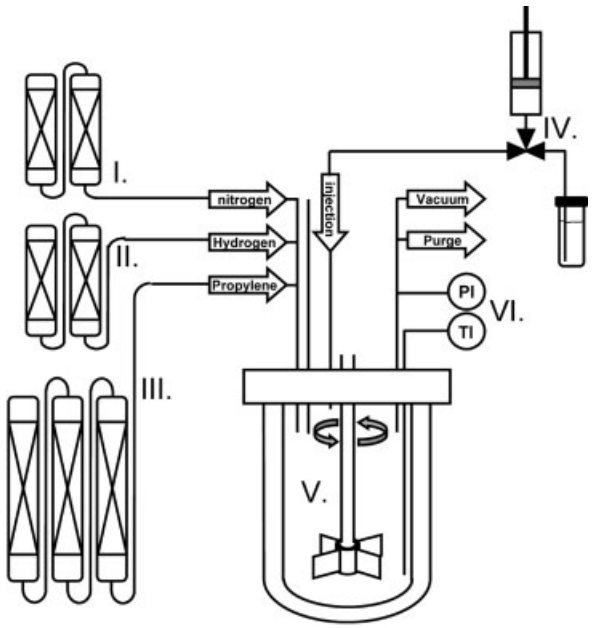

Figure 3 The polymerization setup represented schematically. The setup is described in large detail in previous work [27]: I., II, and III. Gas purification sections for N_2, H_2, and propylene (PPY), IV. Catalyst injection system, V. Polymerization reactor, VI. Data acquisition section.

ter the first injection, the catalyst was injected into the liquid propylene. This vial was also washed twice. Injection of the catalyst started the polymerization reaction.

After the prescribed polymerization time, typically being 75 min, the reaction was stopped by opening the vent valve, allowing the unreacted monomer to evaporate quickly. After flashing and flushing with nitrogen several times, the reactor was opened and the product was dried overnight in a vacuum oven at 80°C.

Prepolymerization method

Three different types of experimental procedures with respect to the prepolymerization step are distinguished. In the first case, no prepolymerization is used at all. The reactor is prepared at the main polymerization temperature and the content of the two vials is injected at this temperature.

In the second case a fixed prepolymerization for 10 min at 40°C was used. Here the reactor was prepared at prepolymerization temperature, the components were injected, and after 10 min the reactor temperature was raised to the main polymerization temperature as quickly as possible. Typically this takes about 3 min.

In the last case, a so-called nonisothermal prepolymerization (NIPP) was used. Here the reactor was prepared at 20°C. The TEA/donor was injected and after injection the reactor temperature was raised to 70°C. During heating, the catalyst was injected at a predefined temperature, resulting in a short prepolymerization step at a varying temperature (increasing from injection temperature to main polymerization temperature).

In this paper we refer to these three prepolymerization methods by the terms "none," "fixed," and "NIPP" respectively. In the NIPP case, it comes with the used injection temperature, or T_{inj}.

Powder characterization

Bulk density

The bulk density was determined using a standardized method of weighting a known loosely packed polypropylene powder. The test method is according to the Japanese Industrial Standard (JIS) K6721. The set up consists of a supported funnel, placed above a receiver. About 120 mL powder is pored through the funnel into the receiver. This receiver is a cylinder with a precisely known volume of about 100 mL. Excess of powder is removed and the filled cylinder is weighed. The bulk density is indicated in gram polymer per liter volume.

Particle size analysis

The particle size distribution of the polymer was measured by laser diffraction. About 5 g of polymer was analyzed by a SympaTec HELOS Laser Diffraction in combination with a Rodos T4 powder disperser. *Windox* software calculated the complete particle size distribution using the Fraunhofer High Reliability Laser Diffraction calculation and provided values for x_{50}, x_{10}, and x_{90} as well as mean particle size values.

Surfacial SEM pictures

SEM was used to visualize details on the surface of the produced polymer particles. The PP powders were mounted on aluminum stubs via double-sided conductive carbon tape and sputter coated with gold to make them conductive. Secondary electron images were taken at represented regions of the specimens via a Philips 505 SEM operating at a working distance of 12 mm. The magnifications and accelerating voltage used in the imaging are shown in the pictures.

Cross-sectional SEM pictures

Some powders produced in slurry prepolymerization were analyzed using SEM imaging on a cross sectional area after cutting of particles. These investigations were done using a Philips environmental scanning electron microscope XL-30 ESEM FEG (Philips, Eindhoven, The Netherlands) equipped with energy dis-

TABLE II
Typical Recipes Used in the Polymerization Tests in This Work[a]

Experiment Type	Hydrogen Amount (mole)	Prepolymerization		Main polymerization	
		T_{prepol}[b] (°C)	Duration (min)	T_{main}[b] (°C)	Duration (min)
No prepol	var: 0–0.069–0.21–0.66	—	—	40–50–60–70–80	75
Fixedprepol	var: 0–0.069–0.21–0.66	40	10	40–50–60–70–80	75
NIPPprepol	var: 0–0.069–0.21–0.66	40–50–60	Short	70	75

[a] Typically 10 mg of catalyst was used A1/Ti = 735, A1/Si = 45.
[b] prepol: Prepolymerization step; main: main polymerization step; *T*: temperature (K).

persive x-ray spectrometer (EDX) for local and area distribution analyses of elements. Secondary electron imaging of the sample surfaces was performed in high vacuum mode using acceleration voltages of 1 kV, whereas qualitative EDX analysis was carried out in wet-mode at accelerating voltages of 5, 10, and 20 kV, respectively. In both cases, no additional coating of the sample surface was done because charging is not an issue for the chosen imaging conditions. For an acceleration voltage of 1 kV, the penetration of the incident electron beam is on the order of a few tens of nanometers for the investigated materials. Therefore, in addition to standard high acceleration voltage scanning electron microscopy, SE images acquired at 1 kV acceleration voltage show surface features in more detail, even at high magnification, whereas the wet mode renders EDX analysis without coating of nonconductive samples unnecessary.

To obtain cross-sectional pictures of the polymer particles, the samples were embedded in epoxy resin and cut at room temperature.

RESULTS AND DISCUSSION

Influence of polymerization temperature

A number of polymerization tests were carried out at various temperatures. The recipes and procedures used are shown in Table II. Temperatures were varied from 40 to 80°C and the catalyst used was not preactivated. This means that, directly after injection of the catalyst into the liquid monomer, the dissolved donor–alkyl complex in the reactor activates the catalyst under polymerization conditions. Figures 4(e–h) show SEM pictures of polymer samples produced at four different polymerization temperatures (40, 50, 60, and 70°C) in the presence of hydrogen.

It is immediately clear that the morphology of the particle is strongly related to the temperature of the polymerization. The particle shapes follow a clear trend from dense, low porosity particles with smooth surface structures, toward the open, irregular shaped particles with low densities produced at high temperatures. The powder morphology shows a continuous gradual change of structure. This is also supported by porosity and bulk density measurements. The series indicated with a square-shaped marker in Figure 5 shows these values for the powders in Figure 4(E–H) (produced at 40, 50, 60, and 70°C, with 0.21 mole hydrogen). With increasing polymerization temperature, bulk densities of the produced powders are rapidly decreasing from the maximum value of about 450 g/L, to the lowest values around 350 g/L. Theoretically the maximum bulk density of spherical polymer particles of identical size, with a crystallinity of about 60% would be 500 g/L, but these values are often not reached, as the particles are not perfectly spherical.

There are different explanations for the influence of polymerization temperature:

- Local Boiling. The change in temperature causes a change in reaction rate in the particle. At higher polymerization rates it is possible that the particle overheats due to insufficient heat transfer. This overheating can lead to the sudden formation of a gas bubble. The force of the gas expansion can cause the surface to form a more open structure.
- Rate of Fragmentation. A higher temperature causes a higher reaction rate in the particle. As fragmentation of the support material is caused by a buildup of internal pressure of polymer on the pore wall; a too rapid increase in this pressure could force the support to fragment in an uncontrolled way, resulting in powders as shown in Figure 4(H).
- Softening of the Polymer. The higher temperature causes a change in the physical properties of the polymer itself. At high pressures, high temperatures, and to some extent the swelling with monomer, the polymeric material will be more soften and more sensitive to changes in shape, caused by shear stresses working on the polymer.

Of course, one can also think about a combination of one or more effects described above. To systematically investigate the effects, a similar series of polymerization tests was done, at different polymerization temperatures, but after a constant prepolymerization step.

The effect of prepolymerization

A series similar to the temperature series was done, but with the use of a so-called fixed prepolymerization

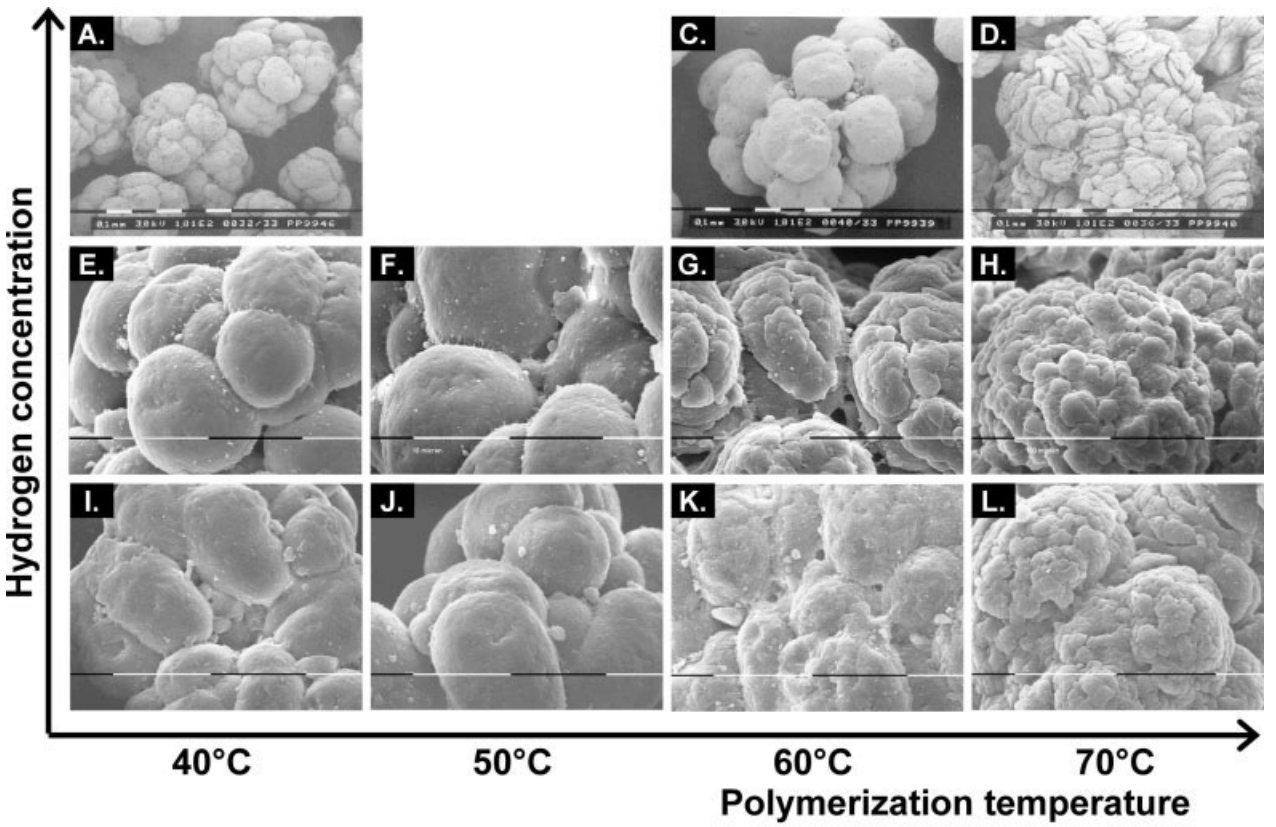

Figure 4 SEM pictures of powders produced without a prepolymerization step, at different polymerization temperatures and different hydrogen concentrations. (White bar indicates 100 μm, in F it indicates 10 μm.)

step. The unactivated catalyst was injected into liquid monomer at a temperature of 40°C. The prepolymerization step was continued for 10 min and then the reactor temperature was raised to the final, main polymerization temperature, which was varied from 40 to 70°C.

Figures 6(E) to 6(H) show the SEM pictures of the four polymer samples taken from those tests. The difference with the case without prepolymerization is remarkable. All particles are very similar, and powder morphology does not seem to be influenced by main polymerization temperature at all. All powders show

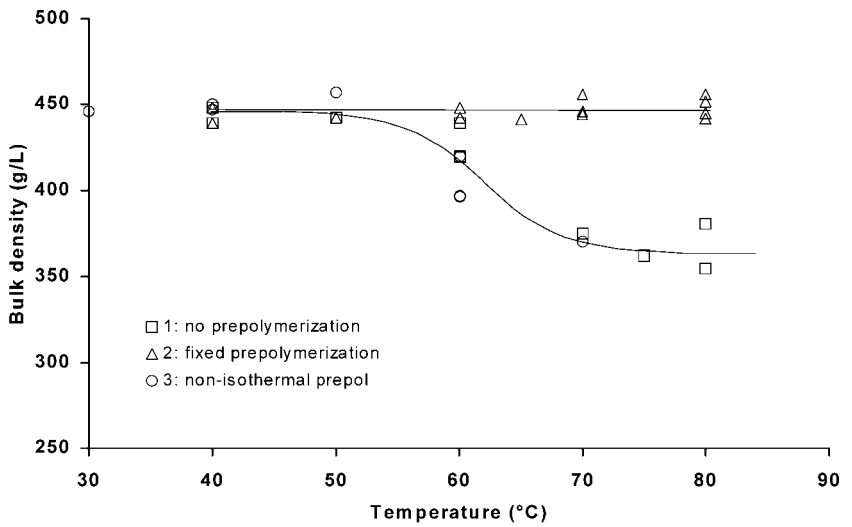

Figure 5 Bulk density as a function of polymerization temperature for series of experiments without, with a fixed, and with a nonisothermal prepolymerization step. In the case of the NIPP, the temperature at the x axis corresponds to injection temperature.

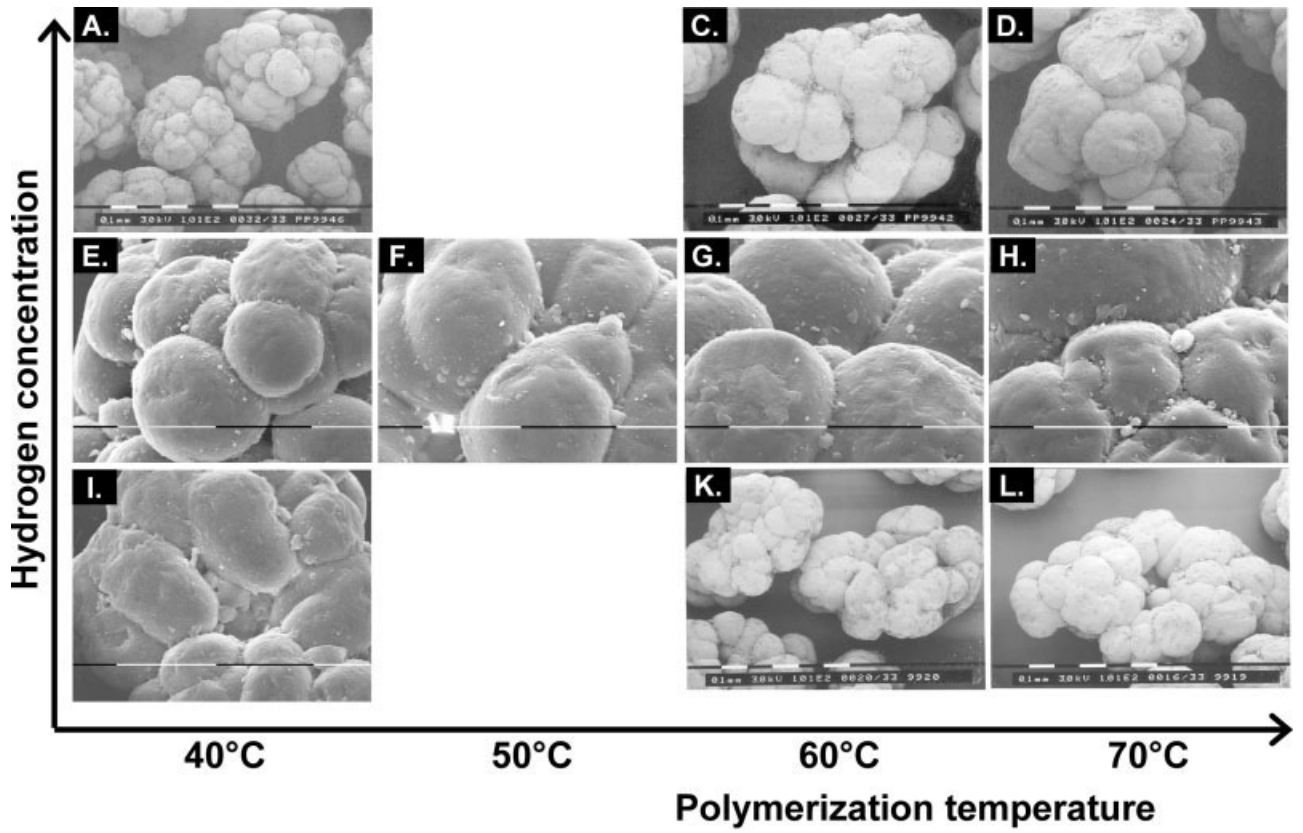

Figure 6 SEM pictures of powders produced with a fixed prepolymerization step of 10 min at 40°C, at different temperatures in the main polymerization and different hydrogen concentrations. (In all pictures, the white bar indicates 100 μm.)

the same morphology as the one shown in Figure 4(E), produced without a prepolymerization step at 40°C. When comparing the particle shape to the shape of the catalyst particles, one can conclude that shape replication is almost perfect.

The observations in SEM are fully supported by the results of porosity and bulk density measurements, as shown in Figure 5. The triangle shaped markers indicate the temperature series including a fixed prepolymerization step as described above. The bulk density of the powders remains a completely stable value of 450 g/L, for all polymer samples. The main polymerization temperature is not influencing this at all.

We previously showed[27] that the final stage of the polymerization, i.e., reduction of reactor temperature, flashing of the unreacted monomer and drying of the powder, in no way influences the particle morphology. From this, we can conclude that the morphology of the particles is determined in the initial stage of the polymerization process.

The first explanation that we mentioned above for the changing morphology is not obvious. If the sudden formation of gas bubbles were causing the open particle structure one would expect "two cases in morphology." In the first case the gas bubbles were formed and the particle was opened up. In the other case thermal runaway did not occur, therefore no bubbles were formed and thus particles were regularly shaped. What can be seen is a gradual change in morphology and thus the first mentioned explanation is not acceptable.

To investigate further these phenomena, the so-called nonisothermal prepolymerization step was applied. The reactor was prepared at 20°C, the donor–alkyl mixture was injected and the reactor temperature was increased. During heating up of the reactor, the unactivated catalyst was injected at a predefined temperature, leading to a short prepolymerization at an increasing temperature. Temperature during the main polymerization was 70°C in all cases. Injection temperature of the catalyst was varied from 30 to 70°C.

Figures 7(D) to 7(F) show the SEM images of the powders yielding from experiments including a nonisothermal prepolymerization step. It can be seen that the morphology of the powder produced with the longest prepolymerization (starting at the lowest temperature, being 30°C) shows a particle shape very similar to the particles produced with a fixed prepolymerization. But when increasing the injection temperature, and with that shortening the prepolymerization period and increasing the initial reaction rate that the particle experiences, the structure of the particle's surface opens up and comes to a situation close to a nonprepolymerized particle.

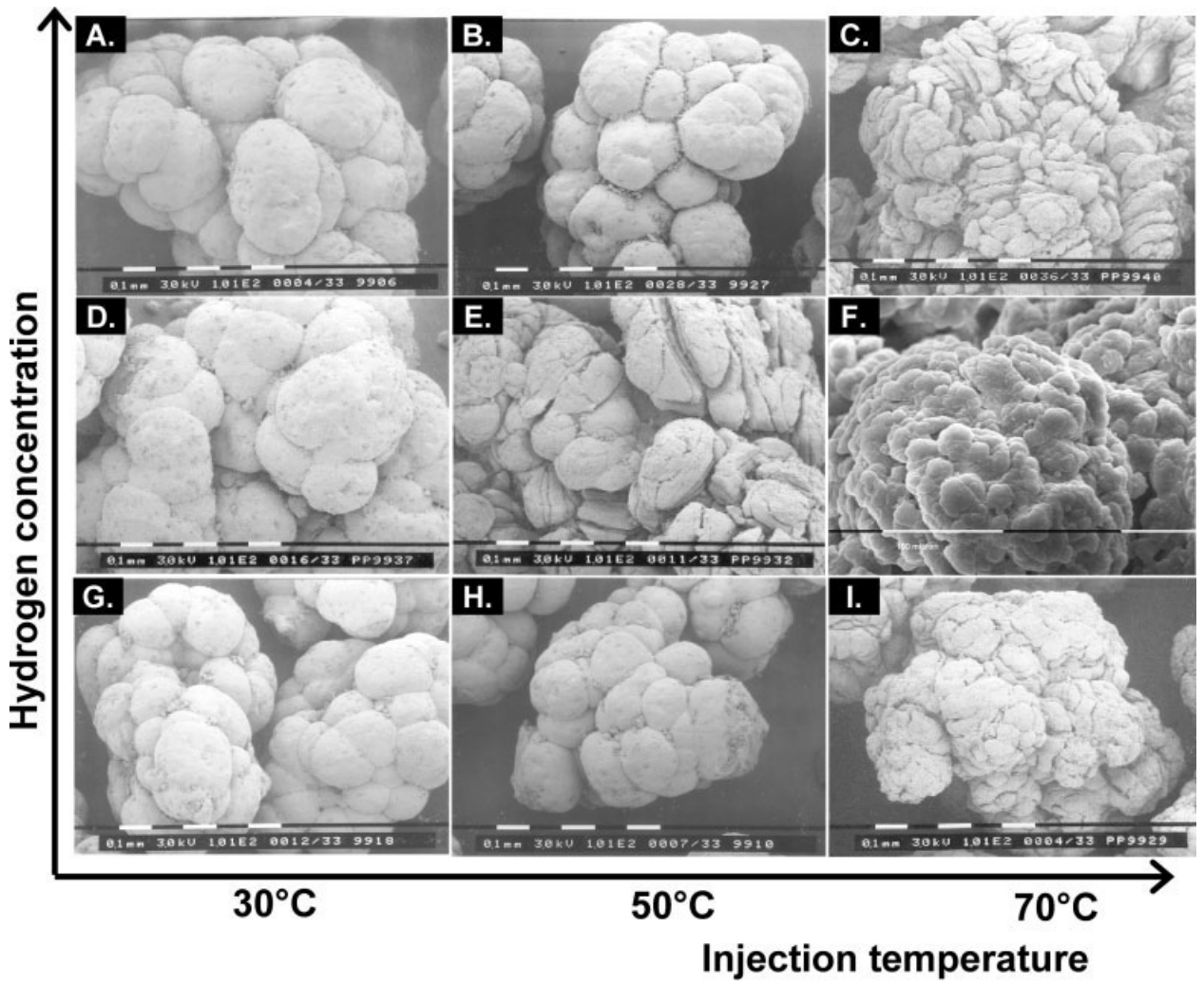

Figure 7 SEM pictures of powders produced without a NIPP prepolymerization step, at different catalyst injection temperatures and different hydrogen concentrations. (In all pictures, the white bar indicates 100 μm.)

This shows that not only the reaction conditions during the main polymerization determine the morphology of the final powder, but also that it is really the process conditions in the first stage of the reaction, that determine how the particle forms and what it will look like. Again, this is supported by the measurements of the bulk density. The circular markers in the plot of Figure 5 show the bulk densities of the powders yielding from the nonisothermal prepolymerization experiments. It is clear that the experiments with longer prepolymerizations, starting at lower initial temperatures, show higher bulk densities.

Influence of hydrogen concentration

Many studies have been carried out to try to understand the influence of the hydrogen on the kinetics and molecular weight in olefin polymerization with Ziegler–Natta catalysts. But it is interesting to see what the addition of hydrogen changes in the morphology of the powder that is produced. Does the influence of the hydrogen on the molecular weight and polymerization rate affect the processes that determine the powder morphology?

The hydrogen concentration during polymerization was varied over a wide range, at different temperatures. This variation was introduced by varying the amount of added hydrogen in the batch experiments targeting at hydrogen amounts of 0, 0.21, and 0.63 moles. In a previous paper we described the vapor–liquid equilibria of the hydrogen–propylene system in more detail. Table III shows the gas and liquid concentrations at different temperatures at the various hydrogen amounts.

The variations in hydrogen concentration were performed for all three types of prepolymerization (none, fixed, and NIPP). The powders resulting from these experiments are also shown in Figures 4, 6, and 7 for cases without, with fixed, and with NIPP prepolymerization, respectively, and Figure 8 shows the bulk

TABLE III
Vapor and Liquid Concentrations of Hydrogen in the H_2–PPY System at Different Temperatures and Different Added Amounts of Hydrogen[27]

	30°C		60°C		80°C	
Hydrogen (moles)	Y_{H2}[a]	X_{H2}[a]	Y_{H2}	X_{H2}	Y_{H2}	X_{H2}
0.00	0.0000	0.0000	0.0000	0.0000	0.0000	0.0000
0.069	0.0269	0.0007	0.0116	0.0010	0.0068	0.0012
0.23	0.0837	0.0022	0.0375	0.0032	0.0223	0.0038
0.66	0.2060	0.0062	0.0994	0.0091	0.0611	0.0110

[a] Y: mole fraction in gas phase; X: mole fraction in liquid phase.

density (BD) values for the series without a prepolymerization step.

Figure 6 shows the almost perfect replication of shape for all particles. When a fixed prepolymerization step was used, the replication of shape for all particles was almost perfect, bulk densities were high, and porosities were low. When comparing Figures 6(D), 6(H), and 6(l), we see that changes in the hydrogen concentration do not influence the particle morphology, at least not at the scale observed here with SEM and BD measurements.

But when no prepolymerization step is used, as shown in Figure 4, the hydrogen concentration clearly effects the morphology of the powder. Powders produced in the absence of hydrogen seem to show the same effect as the powder in the presence of some hydrogen: with increasing polymerization temperature, the surface of the particles is becoming more irregular, and the substructures from which the particles are built become smaller. But this effect seems to start at higher temperatures than when hydrogen is present. At 60°C, the experiment with hydrogen included shows significant changes in particle shape [shown in Fig. 4(G)], whereas in the absence of hydrogen this effect only starts at 70°C. The same is true when larger amounts of hydrogen are used. The addition of more hydrogen does not significantly influence the particle morphology. This gives the impression that the morphology of the particles is to a large extent determined by reaction rate, rather than by some specific reaction conditions. Including the results of the experiments with the NIPP prepolymerization step, we can refine this observation as follows: "the particle morphology is determined to a large extent by the *initial* reaction rate that the particle experiences in its polymerizing life."

Figure 9 shows the correlation between the bulk density and the initial reaction rate that the particle experiences. The reaction rates in the initial stage presented here are extrapolated rates from the reaction rates in the complete experiment and are taken from the kinetic work that we published before.[29] In the case of a nonisothermal prepolymerization, the reaction rate used in this graph is the reaction rate at the temperature of the system at the moment of injection (based on the kinetics [29]).

In this figure the experiments, without, with fixed, and with nonisothermal prepolymerization are in-

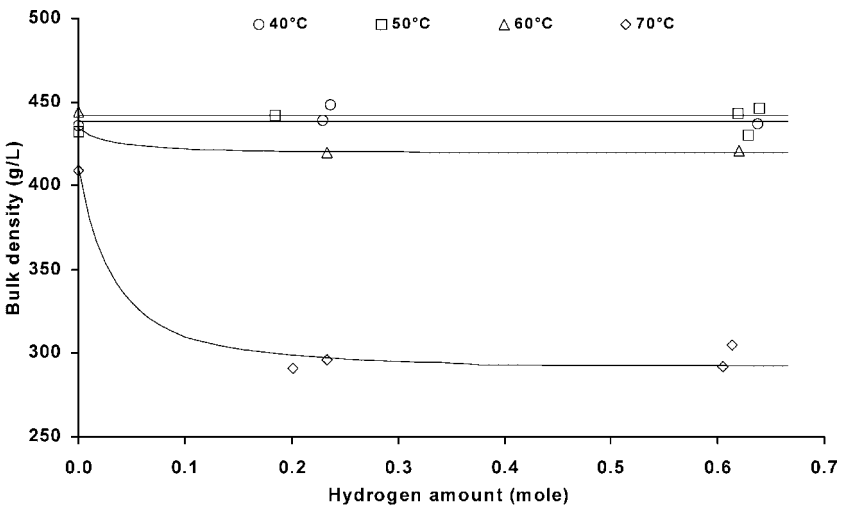

Figure 8 Bulk density of the resulting powders, as a function of the hydrogen concentration in the polymerization experiment for series of different polymerization temperatures. In none of the plotted tests was a prepolymerization step used.

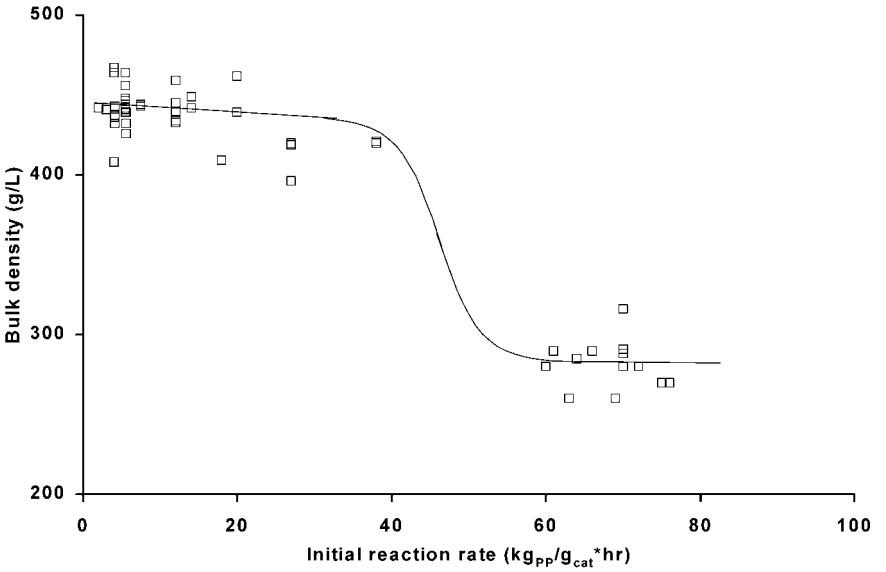

Figure 9 Bulk density of the polymer powder as a function of the initial reaction rate. All types of experiments (no, fixed, and NIPP prepolymerization) are included here. In case of NIPP, reaction rate at T_{inj} (inj: injection) is used, calculated from kinetics of this catalyst.[29]

cluded. It seems to be clear that initial reaction rate is indeed the key factor in determination of the powder morphology. When initial reaction rates are low, bulk densities are always high, and close to the maximum reached value of 450 g/L. With increasing initial reaction rate, the bulk density decreases, toward the lowest observed values of about 250 g/L at initial reaction rates above 60 kg_{PP}/g_{cat} h.

The most likely explanation is that the influence of the initial reaction rate on the morphology of the final polymer particles is caused by the influence of the reaction rate on the fragmentation of the catalyst support. Figures 10(A) to 10(D) (taken from ref. 1) show the development of the internal particle structure of a polymer particle produced with the same catalyst, at very low reaction rates (between 1 and 5 g_{PP}/g_{cat} h). In

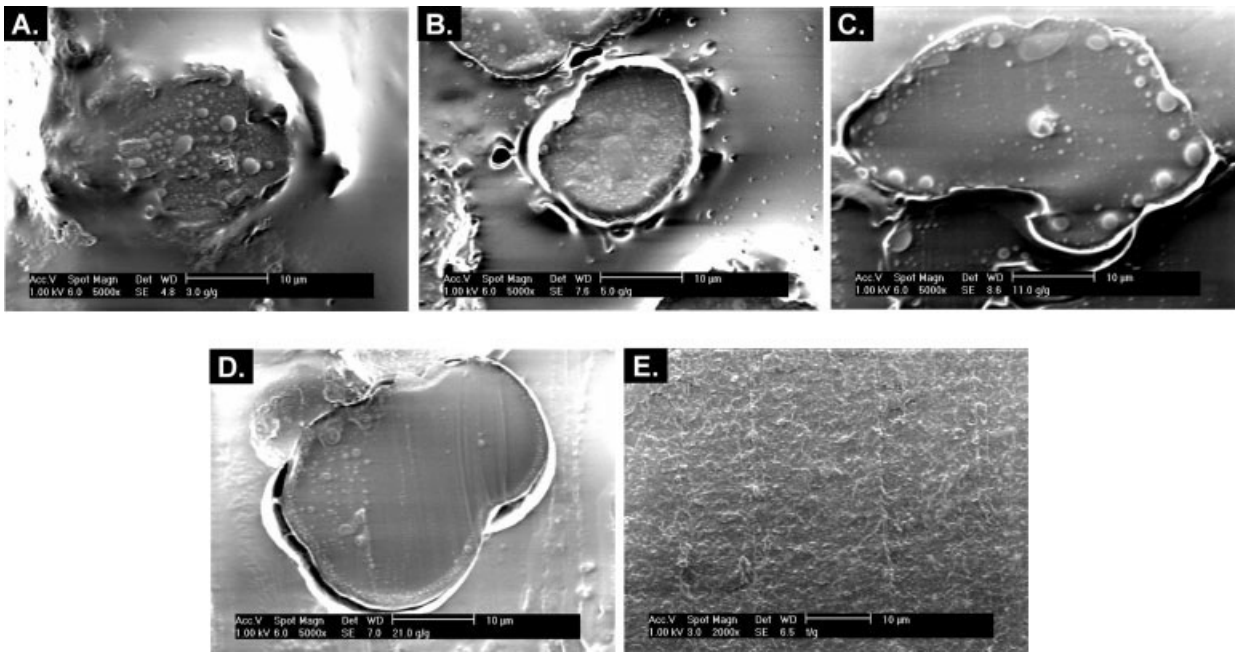

Figure 10 A–D: SEM pictures of a cross-sectional cut of prepolymer particles, produced at very low polymerization rates, with the following values for degree of prepolymerization: A, 3; B, 5, C, 11; D, 21. E: Cross-sectional SEM picture of final polymer powder at high catalyst efficiency of about 40 kg_{PP}/g_{cat}. (All five pictures taken from ref. 1.)

TABLE IV
Typical Polymerization Times Necessary for Reaching the Given Yield in Prepolymerization, for the Presently Used Catalyst at 40 and 70°C

Temperature (°C)	$R_{p,0}$[a] (kg_{PP}/g_{cat} h)	Typical Polymerization Time (s)				
		CE = 3	CE = 5	CE = 11	CE = 21	CE = 50
40	5	2.2	3.6	7.9	15	36
70	70	0.15	0.26	0.57	1.1	2.6

[a] Subscript zero: initial, at time = 0.

these pictures the continuous dark-colored phase is the polymeric material and the heterogeneous, light-colored phase is the catalyst support material, as was concluded from EDX measurements. It can be seen that in the initial stage, polymerization starts throughout the complete particle. The polymer formed in the center of the particle will cause the catalyst support to crack also in the center of the particle and not only at the outside of the particle, as often has been assumed. Figure 10(A) shows a nice distribution of support material over the radius of the particle. With increasing degree of prepolymerization, the fragments get smaller and smaller, until they disappear below the resolution of the electron microscope used here. Figure 10(E) shows a SEM picture of the cross-sectional area of a polymer particle after the main polymerization, with a yield of about 40 kg_{PP}/g_{cat}.

When the reaction rates are higher in the initial stage of the polymerization, the "phase transition" of the particle from catalyst-with-polymer to polymer-with-catalyst is changed as the rate of polymer formation and rate of catalyst fragmentation are changed. At higher initial reaction rates the particle is not able to start fragmentation of the support evenly over the complete particle. When this fragmentation is uneven throughout the particle, the shape of the original catalyst particle will not fully replicate, leading to the shape as shown in, for example, Figure 4(H).

To prove this, one should be able to carry out polymerizations with this same catalyst in liquid propylene at various polymerization temperatures, and stop it at very low yields. Table IV shows typical reaction times for polymerizations at 40 and 70°C resulting in powders with yields in prepolymerization between 3 and 50 g_{PP}/g_{cat}. As these extremely short residence times cannot easily be reached in a batch tank reactor, one should use, for example, stopped-flow type of methods to start and stop the polymerization within a few tenths of a second. Powders from such tests would give new information on the difference in fragmentation between different rates of polymerization.

The effect of the monomer concentration

If the morphology is indeed determined to a large extent by the (initial) rate of polymerization, then one should expect that the effect of reducing the monomer concentration would be similar to the effect of reducing the polymerization temperature. To check this effect, a series of experiments was done at reduced monomer concentrations, without a prepolymerization step. This reduction was provided by replacement of a variable part of the liquid monomer by hexane. By using hexane instead of propylene, the total liquid volume was kept in the same range as the liquid volume in the pure propylene case. So here, the polymerization conditions were gradually changed from bulk liquid pool polymerization toward dilute slurry polymerization in hexane. Of course one has to keep in mind that, in addition to monomer concentration in bulk, more factors are changed by the addition of the hexane. At higher reaction rates and lower catalyst porosity, the presence of inert components can lead to enrichment of this component in the particle. Because of the relatively high molecular weight of hexane, this becomes even more important. (Even simple calculations show that the hexane is not able to diffuse against the convective monomer flow.) Also, the hexane will be sorbed in the polymer, leading to swelling and influencing crystallization of the polymer.

As the reduction of the monomer concentration is expected to decrease reaction rate and a decreased initial reaction rate has been shown to correlate directly with a more regular powder morphology, a reduction of the monomer concentration should increase bulk densities and improve the replication of the shape of the catalyst particles. Figure 11 shows the bulk densities of the powders yielding from this series. It is clear that the bulk density shows a minimum around 300 g/L and goes up again at lower concentrations. The SEM pictures of these powders give more insight in this unexpected result. Figures 12(A) to 12(F) show a series of pictures from the highest to the low monomer concentrations. In the pictures it is clear that all particles look similar, but the particles seem to break up in smaller particles. Figure 12(F), for example, at a C_m of 48 g/L, shows clearly bimodality in the particle size distribution. The sample consists of two types of particles: the particles that are not yet broken and the smaller particles yielding from breaking of the particles.

In a previous study,[29] we examined the relation between the monomer concentration and the observed

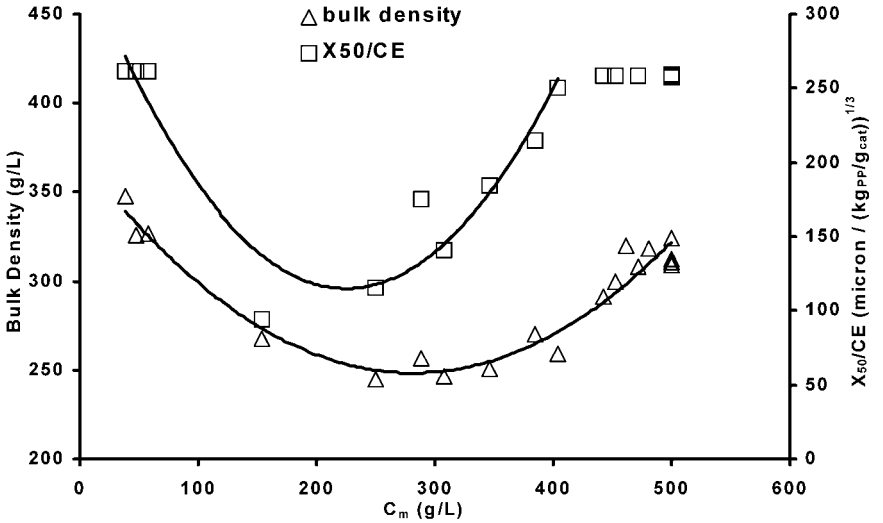

Figure 11 Bulk density of final powder and the ratio of particle size and catalyst efficiency as a function of monomer concentration in main polymerization. Concentration of propylene was reduced by addition of hexane to the liquid monomer.

reaction rates. It was shown there that the reaction rate did not, as would be expected from the usual kinetic models, decrease linearly with decreasing monomer concentration. Rather, contrarily to what one would expect from eq. (1), it was more or less constant when the monomer concentration decreased from 500 down to a value of about 200 g/L.

$$R_p = k_p \cdot (C_m)^q \cdot C^* \quad (1)$$

where R_p is the reaction rate of polymerization (kg_{PP}/g_{cat} h), k_p is the propagation rate constant (L/mole h), C_m is the concentration of monomer, (g/L), q is the order of propagation, and C^* is the concentration of active sites (mole/g). Decreasing monomer concentration any further, below this concentration, caused a sudden drop of reaction rate.

The apparent bimodality of the particle size distribution (PSD) seen in the SEM images is fully supported by particle size measurements shown in Figure 13. It is clear that with reducing monomer concentration, the relatively narrow PSD develops to lower particle sizes and at a certain moment toward bimodality. At really low C_m, the bimodality disappears and a low particle size (PS) remains. Of course the low reaction rates at low monomer concentrations also contribute to the change in PS; therefore the ratio between the average particle size and the catalyst efficiency, X_{50}/CE, is added to the plot in Figure 11,

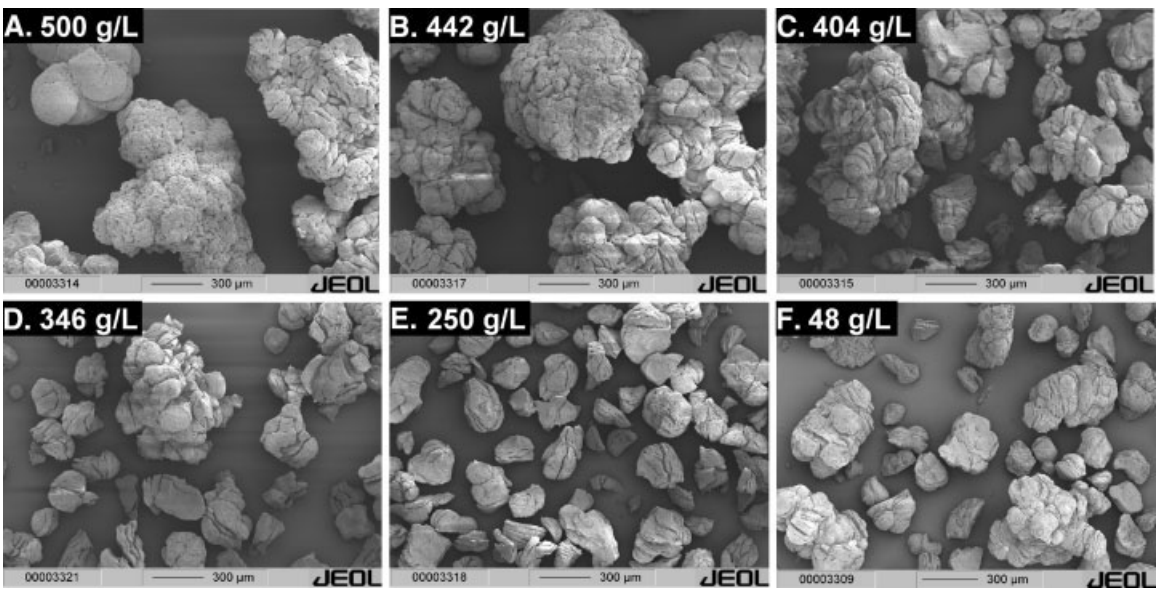

Figure 12 SEM pictures of polymer powders yielding from experiments at various monomer concentration (monomer concentration was reduced by addition of hexane to liquid monomer).

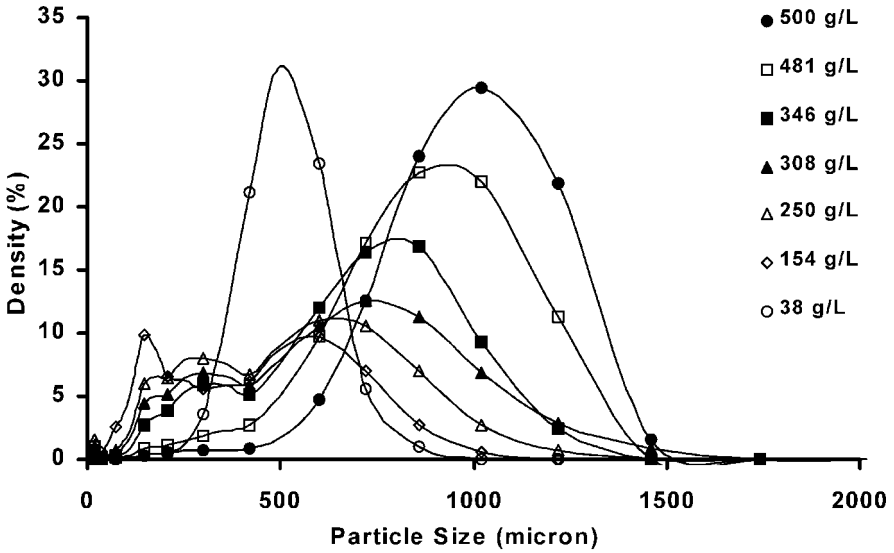

Figure 13 PSD curves for powders produced at varied monomer concentration. It is clear that bimodality appears at lower values for C_m. At the lowest C_m values, this effect has disappeared.

indicated with the square-shaped markers. As expected, it follows the same trend as the bulk density.

A further proof for the fact that the morphology of the particles is indeed determined in the initial stage of the polymerization is given in the SEM pictures of Figure 14. This figure shows powder after a prepolymerization step in liquid propylene and a subsequent polymerization at 70°C at lowered monomer concentration (C_m = 420 g/L). The powder shows a perfect replication of the particle's shape and shows very regular, smooth particle surface. This is a proof that the typical structures formed in the dilute polymerization are annulled by the prepolymerization in liquid propylene at lowered temperature and the main polymerization in hexane-diluted monomer does not lead to typical structures coming with this dilution.

CONCLUSIONS

Many factors determine the morphology of the polymer powder. Most of them are expected to influence morphogenesis directly, but the way and type of this effect is often not understood. The fragmentation of the catalyst support plays an important role in the formation of the particle shape, especially regarding the nature of the polymerization reaction and the initial (fragmentation) stage.

Next to that, the state of the polymer formed, influenced by temperature, swelling with monomer, and polymer properties like tacticity and mole weight can determine the particle's structure.

In the present work it has been shown experimentally that the initial reaction rate is the crucial factor in

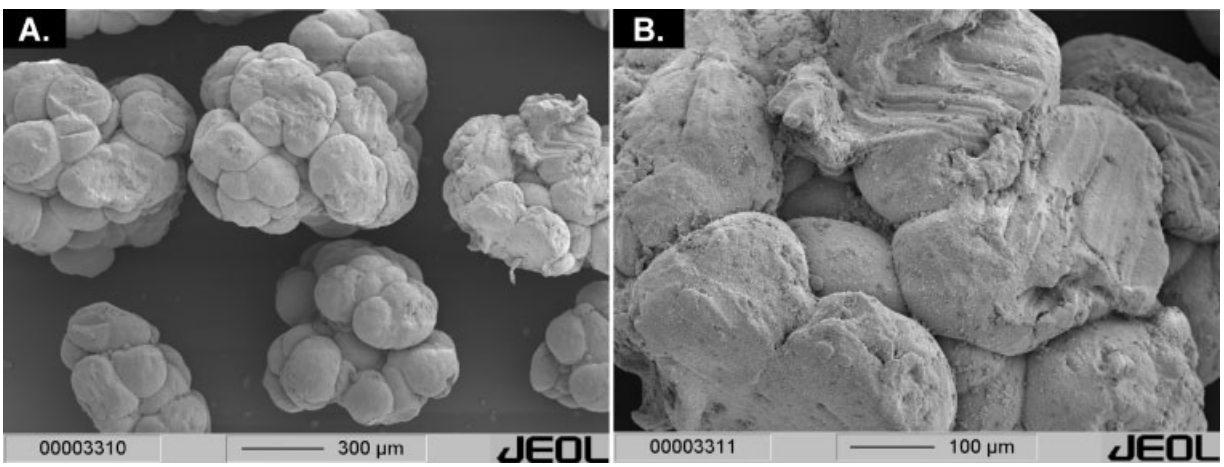

Figure 14 SEM pictures of powder produced at reduced monomer concentration (C_m=420 g/L) after a prepolymerization step in liquid monomer of 40°C for 10 min. (Picture B is an enlargement of picture A.)

the development of the shape of the polymer particle. The influence of other parameters like temperature, pressure, and hydrogen concentration can be traced back to their influence on the initial rate. When this rate is high, the particle will not be able to replicate the shape of the catalyst particle, will form irregularly shaped surface structures, will show high porosities, and will show low values for bulk density. A short prepolymerization, lasting no longer than 1 min at an increasing polymerization temperature—or polymerization rate— is often sufficient to effect that the particle will show a high density and that the shape of the particle will be very regular while a perfect reproduction of the catalyst particle is realized.

It was shown that for the catalyst system investigated here, the nonisothermal prepolymerization is a good option for prepolymerization purposes. In industry often either a continuous stirred reactor is used for prepolymerization, resulting in broad residence time distributions, or a batch tank reactor is used, resulting in a laborious and expensive prepolymerization. When using a tube plug flow reactor with a residence time up to some minutes operated at an increasing axial temperature profile (starting at room temperature and ending at the main polymerization temperature), a satisfactory solution for prepolymerization will be obtained.

Finally, it can be concluded that to understand the fragmentation process and the other processes playing a role in the development of the particle morphology, also at higher reaction rates (e.g., without prepolymerization), one should solve the experimental problem of following polymerizations at high polymerization rates.

The work presented in this paper was carried out in cooperation with The authors thank Dow for both the financial and the intellectual input. The aluminum alkyls used in the work were kindly donated by AkzoNobel, Deventer, The Netherlands. In addition, the technical assistance of Gert Banis, Fred ter Borg, Karst van Bree, and Geert Monnink is highly appreciated.

References

1. Pater, J. T. M.; Weickert, G.; Loos, J.; van Swaaij, W. P. M. Chem Eng Sci 2001, 56, 4107.
2. Galli, P.; Barbe, P. C.; Noristi, L. Angew Makromol Chem 1984, 120, 73.
3. Galli, P.; Luciani, L.; Cecchin, G. Angew Makromol Chem 1981, 94, 63.
4. Galli, P.; Haylock, J. C. Progr Polym Sci 1991, 16, 443.
5. Galli, P.; Haylock, J. C. Makromol Chem Macromol Symp 1992, 63, 19.
6. Sasaki, T.; Ebara, T.; Johoji, H. Polym Adv Technol 1993, 4, 406.
7. Albizzati, E.; Galimberti, M. Catal Today 1998, 41, 159.
8. Floyd, S.; Heiskanen, T.; Taylor, T. W.; Mann, G. E.; Ray, W. H. J Appl Polym Sci 1987, 33, 1021.
9. Nagel, E. J.; Kirillov, V. A.; Ray, W. H. Ind Eng Chem 1980, 19, 372.
10. Floyd, S.; Choi, K.Y.; Taylor, T. W.; Ray, W. H. J Appl Polym Sci. 1986, 32, 2231.
11. Floyd, S.; Choi, K.Y.; Taylor, T. W.; Ray, W. H. J Appl Polym Sci 1986, 32, 2935.
12. Hutchinson, R. A.; Chen, C. M.; Ray, W. H. J Appl Polym Sci 1992, 44, 1389.
13. Ferrero, M. A.; Chiovetta, M. G. Polym Eng Sci 1987, 27, 1436.
14. Ferrero, M. A.; Chiovetta, M. G. Polym Eng Sci 1987, 27, 1448.
15. Ferrero, M. A.; Chiovetta, M. G. Polym Eng Sci 1991, 31, 904.
16. Ferrero, M. A.; Chiovetta, M. G. Polym Eng Sci 1991, 31(12), 886.
17. Ferrero, M. A.; Koffi, E.; Sommer, R.; Conner, W. C. J Polym Sci, Polym Chem 1992, 30, 2131.
18. Noristi, L.; Marchetti, E.; Baruzzi, G.; Sgarzi, P. J Polym Sci Polym Chem 1994, 32, 3047.
19. Kakugo, M.; Sadatoshi, H.; Sakai, J.;Yokoyama, M., Macromolecules 1989, 22, 3172.
20. Kakugo, M.; Sadatoshi, H.; Yokoyama, M.; Kojima K. Macromolecules 1989, 22, 547.
21. Ferrero, M. A.; Sommer, R.; Spanne, P.; Jones, K. W.; Conner, W. C. J Polym Sci Polym Chem 1993,31, 2507.
22. Han-Adebekun, G. C.; Hamba, M.; Ray, W. H. J Polym Sci Polym Chem 1997, 35 (10), 2063
23. Han-Adebekun, G. C. Ph.D. thesis, Department of Chemical Engineering, University of Wisconsin, Madison, WI, 1996.
24. Cecchin, G.; Marchetti, E.; Baruzzi, G. Macromol Chem Phys 2001, 202(10), 1987.
25. Kittilsen, P.; McKenna, T. F. J Appl Polym Sci 2001, 82, 1047.
26. Moore, E. P. Polypropylene Handbook; Hanser: Munich—Vienna—New York, 1996.
27. Pater, J. T. M.; Weickert, G.; van Swaaij, W. P. M. AIChE J 2003, accepted for publication.
28. Shimizu, F.; Pater, J. T. M.; Weickert, G.; van Swaaij, W. P. M. J Appl Polym Sci 2001, 81, 1035.
29. Pater, J. T. M.; Weickert, G.; van Swaaij, W. P. M. Chem Eng Sci 2002, 57, 3461.